Article

Advanced Method of Variable Refrigerant Flow (VRF) System Design to Forecast on Site Operation—Part 3: Optimal Solutions to Minimize Sizes

Mykola Radchenko [1] , **Andrii Radchenko** [1], **Eugeniy Trushliakov** [2], **Anatoliy Pavlenko** [3,*] and **Roman Radchenko** [1]

1   Machinebuilding Institute, Admiral Makarov National University of Shipbuilding, Heroes of Ukraine Avenue 9, 54025 Mykolayiv, Ukraine
2   Department of Air Conditioning and Refrigeration, Admiral Makarov National University of Shipbuilding, Heroes of Ukraine Avenue 9, 54025 Mykolayiv, Ukraine
3   Department of Building Physics and Renewable Energy, Kielce University of Technology, Avenue of 1000 Years of the Polish State, 7, 25-314 Kielce, Poland
*   Correspondence: apavlenko@tu.kielce.pl

Abstract: Outdoor air conditioning systems (ACS) are used as autonomic systems as well as in combined outdoor and indoor ACS of the variable refrigerant flow (VRF) type, with variable speed compressors (VSC) as their advanced version. Methods for determining the optimal value of refrigeration capacity and providing the maximum rate of the summarized annual refrigeration energy generation increment, according to its needs at minimum compressor sizes and rational values, are applied to reveal the reserves for reducing the designed (installed) refrigeration capacity, thus enabling us to practically achieve maximum annual refrigeration energy generation as the primary criterion at the second stage of the general design methodology previously developed by the authors. The principle of sharing the total thermal load on the ACS between the ranges of changeable loads for outdoor air precooling, and a relatively stable load range for further processing air are used as its basis. According to this principle, the changeable thermal load range is chosen as the object for energy saving by recuperating the excessive refrigeration generated at lowered loading in order to compensate for the increased loads, thereby matching actual duties at a reduced designed refrigeration capacity. The method allows us to determine the corresponding level of regulated loads (LRL) of SRC and the load range of compressor operation to minimize sizes.

Keywords: air conditioning system; load range; refrigeration capacity excess; threshold temperature; level of loading

1. Introduction

Ambient air conditioning systems (ACS) are desired to provide comfortable environments in buildings [1,2] and other stationary objects [3,4]. They are widespread in transport application, in particular in railways [5,6] and ships [7,8]. As the air is a working fluid (cyclic air) for combustion, ACS are used for cooling air sucked out of combustion engines, these being internal combustion engines [9,10], gas turbines [11,12] and gas engines [13,14]. The latter are effective in the development of engine intake air conditioning systems as subsystems of trigeneration (in-cycle trigeneration) [15,16] and integrated power plants [17,18] for combined cooling, heat and power (CCHP) generation [19,20]. In these cases, the ACS function as waste heat recovery systems [21,22] and their cooling potential depends on a depth of engine exhaust heat utilization [23,24]; the deeper the exhaust heat utilization, the higher the thermal (refrigeration) potential of the ACS.

Such mutual penetration of ACS into power plants and, conversely, the use of energy heat exhausts as a thermal source for ACS reveal the potential for application of the principal

findings gained in energetic application to ACS. Therefore, evaporative cooling [25,26], two-stage cooling air [27,28] by chilled water and refrigerants coolants [29,30] in hybrid coolers [31,32] and combined chillers of different types [33,34], including absorption [35,36] and refrigerant [37,38] chillers as cascade chillers [39,40], and excessive heat recuperation to cover peak loads [41,42] were implemented into ACS as two-stage outdoor air conditioning systems that use refrigeration recuperation [43,44]; they are especially efficient for combined outdoor and indoor air-processing unites [45,46].

The outdoor unit is desired for conditioning the ambient air in order to avoid fluctuated heat loads and overloading the indoor unit [47,48]. The VRF systems save more than 20% energy compared to the variable air volume ACS [49,50].

A performance of ACS is characterized by off-design modes which are especially evident in temperate climatic conditions and off-season operation. Therefore, the VRF systems are the most well adapted to cover efficient off-season operation [51,52].

The varying heat loads on ACS and heat exchangers accordingly are accompanied by heat flux drops which require application of efficient heat exchangers and working fluid circulation circuits. The application of high-efficiency heat exchangers [53,54], in particular compact evaporators [55,56] and condensers [57,58], accelerates research focused on intensifying heat transfer [59,60] and hydrodynamics [61,62] to mitigate the instabilities of two-phase refrigerant flows [63,64] and uneven refrigerant [65,66] and air [67,68] distribution. Advanced air conditioning, refrigerant feeding and exhaust heat recovery circuits, in particular with the application of ejectors [69,70] and thermopressors [71,72], as circulation devices which use potential energy and exhaust heat [73,74], were developed.

In reality, all the management methods [75,76], criteria [77,78] and indicators [79,80] are required in order to cover varying loads without considerable oversizing.

Methods for determining the rational value of the design refrigeration capacity enable us to achieve practically maximum annual fuel saving [81,82] as well as refrigeration energy generation according to current need, as the primary criterion and its optimal value, providing the maximum rate of the summarized annual refrigeration energy generation increment at minimum compressor sizes, was previously developed by the authors [83,84]. The general methodology of rational designing also includes the rational distribution of the overall current thermal loads in the ranges of changeable loads for ambient air preconditioning, and a relatively stable load range for further air subcooling from a threshold temperature to the set value.

The method for estimating the SRC compressors performance efficiency by comparing the load ranges of regulated and unregulated by SRC with the ranges of changeable and unchangeable loads was developed by the authors earlier. With this, the efficiency of SCR operation is estimated by the loading rate of the unregulated (stable) range assumed as the object of investigation [84].

It is quite evident that the range of unstable (regulated) loads can be accepted as the object for the recuperation of excessive refrigeration to cover the current increased loads that result in the reduction of the range needed for load regulation.

In reality, the SRC is the oversized (underloaded) compressor that operates efficiently at part loads. With a higher level of regulated (changeable) loads (LRL) of the SRC, there is more oversizing of the compressor. It is quite preferable to reduce the SCR sizes through narrowing the range of changeable thermal loads, leading to a decrease in the LRL of the SRC applied. In its turn, in concrete site climatic conditions, the magnitude of the changeable thermal load range depends on the exceedance of the design refrigeration capacity over current loads.

The lesser the exceedance of the design refrigeration capacity (the higher the level of loading LL), the narrower the changeable (booster) thermal load range.

Thus, reduction in the SCR size may be possible due to reduction in the exceedance (excess) of the design refrigeration capacity through its use to cover the pick loads that leads to shortening of the changeable load range due to its part-stabilization [85].

The level of loading LL is a criterion for shearing the total range of loading q_0 to the ranges of changeable $(1 - \text{LL})\, q_0$, and unchangeable $\text{LL}\, q_0$ loads, and is calculated as the ratio of unchangeable load $\text{LL}\, q_0$ to the total load q_0.

The enhancement of the ACS operation efficiency is focused on raising the level of load LL followed by reducing the range of changeable load $(1 - \text{LL})q_0$ while correspondingly growing the range of unchangeable load $\text{LL}\, q_0$.

The maximum rate of the summarized annual refrigeration energy generation increment according to its consumption (as the maximum level of loading LL) is associated with a threshold (optimal) value of refrigeration capacity as the minimum permissible value of the design refrigeration capacity [84].

The further reduction of the design refrigeration capacity to less than its threshold (optimal) value at the maximum rate of the annual refrigeration increment is unreasonable, because it propagates an unchangeable (stable) load range. The operation in the unchangeable load range is characterized by full loading of the compressor and the ACS as a whole (LL = 1).

The rational value that enables us to achieve close to maximum annual refrigeration energy generation as a primary criterion is determined at the second stage of the general design methodology developed by the authors [84].

It is quite evident that an increase in the design refrigeration capacity from its optimal value as a minimum to the rational value, providing maximum refrigeration energy generation in response to current need, is accompanied by widening the changeable (requiring the regulation by SCR) load range and an increase in the exceedance (excess) of the design refrigeration capacity available for recuperation leading to part-stabilization of initially changeable load range for outdoor air preconditioning [85].

Thus, it is quite reasonable to assess the application of both methods to reveal the reserves for reducing the design (installed) refrigeration capacity of ACS and the level of regulated loads (LRL) of SRC, as well as the load range of compressor operation. These reserves can be evaluated by comparing the exceedance of the installed (design) refrigeration energy determined according to both methods and conserved at lowered actual loads with current need. Their realization is made possible by recuperating the excess refrigeration energy to enhance the operation efficiency of the advanced VRF system with modern SRC to minimize the oversizing.

The object of the research is the range of unstable (regulated) loads within the overall range of actual loading as the source of exceedance (excess) of refrigeration to cover the current increased loads, resulting in a reduction in the range of necessary load regulation.

The aim of the research is to reveal the reserves for reducing the design (installed) refrigeration capacity of ACS, determined by different methods, to provide maximum annual refrigeration energy generation or a maximum rate of its increment (rational and optimal values), and to realize them through recuperation of the excessive refrigeration to cover the current increased loads, resulting in a reduction in the range of unstable (regulated) loads, the level of regulated loads (LRL) of SRC and the load range of compressor operation.

The following tasks are to be solved to reach these aims:

- Determine the ranges of changeable thermal loads for optimal and rational refrigeration capacities of ACS, calculated according two methods of providing the maximum rate of the summarized annual refrigeration energy generation increment, or providing close to maximum refrigeration energy generation;
- Develop a method to determine the range of artificially stabilized loads due to recuperation of excessive refrigeration energy, reserved at lowered current loads, to cover peak loads and the rest of the range of unstable loads regulated by SRC, thereby defining the level of regulated loads (LRL) of SRC and the load range of compressor operation.

These reserves are evaluated by comparing the exceedance of the installed (design) refrigeration energy conserved at lowered actual loads, according to both methods with current need.

2. Methods

In order to generalize the results and adopt their application for ACS of any sizes (refrigeration capacity Q_0 according to air mass flow rate G_a), they are presented in relative values as specific refrigeration capacity q_0, id est, referred to in the unit of air mass flow rate (G_a = 1 kg/s):

$$q_0 = Q_0/G_a, \tag{1}$$

and calculated as

$$q_0 = \xi \cdot c_a \cdot (t_a - t_{a2}), \text{kW}/(\text{kg}/\text{s}), \tag{2}$$

where t_a—initial or ambient t_{amb} air temperature, K or °C;

t_{a2}—a set air temperature;
ξ—relative heat ratio as the total heat, removed from the air, related to its sensible heat;
c_a—air specific heat, kJ/(kg·K).

The summarized annual refrigeration energy generation in response to consumption is accepted as a primary criterion. The corresponding specific annual energy generation is calculated as

$$\Sigma(q_0 \cdot \tau) = \Sigma \xi c_a \cdot (t_a - t_{a2}) \cdot \tau \cdot 10^{-3}, \text{MWh}/(\text{kg}/\text{s}). \tag{3}$$

In order to avoid the errors of about 20% caused by approximation of the actual changeable thermal loads and corresponding required refrigeration capacities, their fluctuations are considered by the rate of their summarized annual value increment versus the refrigeration capacity q_0 used as a cumulative annual refrigeration energy characteristic:

$$\Sigma(q_0 \cdot \tau) = f(q_0). \tag{4}$$

Such an approach allows us to use the rate of their summarized annual values increment in response to refrigeration capacity q_0 as the indicative criterion $\Sigma(q_0 \cdot \tau)/q_0$ to choose the optimal value of refrigeration capacity $q_{0.opt}$ corresponding to its maximum.

The same indicative criterion is applied to determine the precise value of rational refrigeration capacity $q_{0.rat}$ within the range of cumulative annual refrigeration energy characteristics above the optimal value $q_{0.opt}$ to avoid the overestimation of refrigeration capacity accompanied by a negligible increment of annual output.

The values of rational $q_{0.rat}$'s specific refrigeration capacities while conditioning outdoor air were calculated for temperate climatic conditions in southern Ukraine (Mykolayiv region), 2017 (Figure 1).
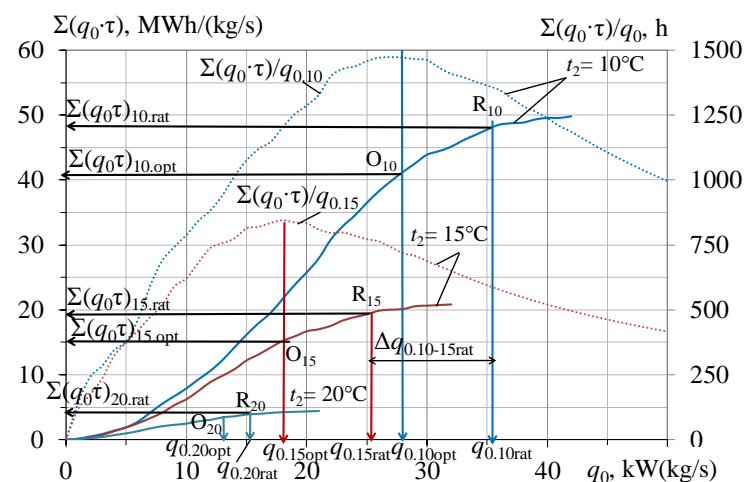

Figure 1. Specific annual refrigeration energy consumption $\Sigma(q_0 \cdot \tau)$, rational $q_{0.rat}$ and optimal $q_{0.opt}$ refrigeration capacities while conditioning air to t_{a2} = 10, 15 °C and 20 °C: $LL_{10rat} = (q_{0.10rat} - q_{0.15rat})/q_{0.10rat}$.

The rational value $q_{0.\text{rat}}$ of the design refrigeration capacity enables us to offset the annual refrigeration consumption $\sum(q_0 \cdot \tau)_{\text{rat}} = 48$ MWh/(kg/s) that is close to its maximum value 50 MWh/(kg/s) but is also achieved at reduced design refrigeration capacity $q_{0.10\text{rat}} = 35$ kW/(kg/s), which is less than $q_{0.10\text{max}} = 42$ kW/(kg/s) (Figure 1).

The level of load (LL) on ACS proceeding from the summarized annual refrigeration energy can be applied as a modified criterion in contrast to the current level of load LL_{cur} used in conventional practice: $LL_{10\text{rat}} = (q_{0.10\text{rat}} - q_{0.15\text{rat}})/q_{0.10\text{rat}} \approx 0.3$, where $q_{0.10\text{rat}} - q_{0.15\text{rat}}$ is the range of stable thermal load and $q_{0.15\text{rat}}$ is the range of changeable thermal loads.

The maximum value of the indicative criterion $\sum(q_0 \cdot \tau)/q_0$ reflects the maximum rate of the summarized annual refrigeration energy increment, and naturally, the minimum deviation of the optimal value of refrigeration capacity $q_{0.\text{opt}}$ from the current loads q_0, followed by minimum exceedances of $q_{0.\text{opt}}$ over q_0. Therefore, the rational value of refrigeration capacity $q_{0.\text{rat}}$, being higher than $q_{0.\text{opt}}$, is characterized by larger deviation from the current loads q_0 and exceedances (excesses) of $q_{0.\text{rat}}$ over q_0. The latter are considered the reserves for refrigeration exceedances (excesses)' recuperation to cover peak loads and reduce a design refrigeration capacity less than $q_{0.\text{rat}}$. The refrigeration exceedances (excesses) are associated with changeable load range of the total one. Therefore, the range of changeable loads is considered the object for partly stabilizing due to refrigeration exceedances (excesses) recuperation that leads to a reduction in its value and the total design refrigeration capacity $q_{0.\text{rat}}$ as result.

The residual part of the range with initially changeable loads becomes considerably narrower than the primary one that leads to reducing the ratio of the changeable load range, covered by the RSC, to the overall load range, id est. the required level of regulated loads (LRL).

3. Results and Discussion

According to the aim of the research, the range of changeable loads is considered as the object for partly stabilizing due to refrigeration exceedances (excesses)' recuperation in order to reduce its value and the total design refrigeration capacity $q_{0.\text{rat}}$ as result. Such an approach, substantiated by the results of calculation of the summarized annual refrigeration energy generation $\sum(q_0 \cdot \tau)$ and optimal $q_{0.\text{opt}}$ and rational $q_{0.\text{rat}}$ refrigeration capacities (Figure 1), should be proven by the exceedances (excesses) of design refrigeration capacities $q_{0.\text{opt}}$ and $q_{0.\text{opt}}$ over current loads q_0, and corresponding monthly summarized values of the refrigeration energy exceedances $\sum(q_0 \cdot \tau)$ within initial changeable load range $q_{0.15}$ reduced by its partially stabilization due to refrigeration energy exceedance's recuperation in the range to $q_{0.20}$.

The total values of specific refrigeration capacities $q_{0.10}$ needed for conditioning outdoor air to 10 °C can be sheared into the range of changeable values $q_{0.15}$, which are needed for preconditioning outdoor air to 15 °C. Practically unchangeable refrigeration capacities $q_{0.10\text{-}15}$ are needed for subsequent conditioning of air from 15 °C to 10 °C. The calculation results for July 2017 in climatic conditions in southern Ukraine, Mykolayiv region, as example of temperate climate, are presented in Figure 2.

As Figure 2 shows, the current total changeable heat load $q_{0.10}$ for conditioning outdoor air to 10 °C can be shared in the range of changeable load for preconditioning outdoor air to 15 °C, and in the range of practically unchangeable heat load $q_{0.10\text{-}15}$ for subsequent conditioning air from 15 °C to 10 °C. Accordingly, the latter is accepted as the basic practically unchangeable part, $q_{0.10\text{-}15} \approx q_{0.10\text{rat}} - q_{0.15\text{rat}}$, of the total rational design value $q_{0.10\text{rat}}$, whereas the rest, as a remainder of the rational design value $q_{0.10\text{rat}}$, might be used as the residual booster one $q_{0.b10\text{-}15} = q_{0.10\text{rat}} - q_{0.10\text{-}15}$, available for preconditioning outdoor air to 15 °C. It is chosen as the object for reduction through refrigeration exceedances (excesses)' recuperation.

Based on the above, the intermediate temperature 15 °C is accepted as a threshold one t_{thr}, stabilizing the heat loads for further conditioning outdoor air below $t_{\text{thr}} = 15$ °C,

and as an indicator to share the overall range of design heat load $q_{0.10rat}$ (Figure 1) in two ranges according to different character of the loading.
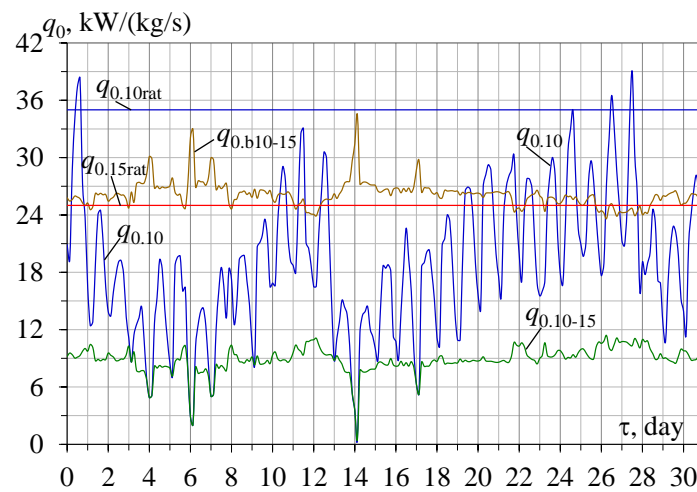

Figure 2. The current values of specific refrigeration capacities $q_{0.10}$ required for outdoor air conditioning to 10 °C; refrigeration capacities $q_{0.10-15}$ for subsequent air conditioning from 15 °C to 10 °C; available booster values $q_{0.b10-15}$ remained for outdoor air conditioning to 15 °C: $q_{0.10-15} = q_{0.10} - q_{0.15}$; $q_{0.b10-15} = q_{0.10} - q_{0.10-15}$.

Issuing from a changeable character of loading and accompanied by inevitable excesses of design refrigeration capacity $q_{0.10rat}$ over actual loads $q_{0.10}$, reflected in the booster refrigeration capacity $q_{0.b10-15} = q_{0.10rat} - q_{0.10-15}$ and available for preconditioning outdoor air to 15 °C, the latter is accepted as the object for analyses in order to use the excess refrigeration capacity for covering the peak loads. Therefore, the next step of the analyses aims to partly stabilize the initially changeable heat loads $q_{0.15}$, which would lead to reduce the booster load range from $q_{0.b10-15}$ to $q_{0.b10-20}$, as the regulated load range and the LRL of SRC compressor recuperate the refrigeration energy exceedance.

Proceeding from the approach to partly offset the current heat load fluctuations due to a reduction in the refrigeration capacity $q_{0.15}$ by using the value $q_{0.20rat}$ to condition air to 20 °C, the latter might be accepted as the artificial threshold temperature $t_{thr} = 20$ °C, and the range of heat loads $q_{0.10-20}$ as the artificially stable range in the initial approximation (Figure 3).

The results of the refrigeration energy exceedance recuperation for covering the booster preconditioning load $q_{0.15}$ using the reduced rational refrigeration capacity $q_{0.20rat}$ are presented in Figure 3.

The following correlations are used: $q_{0.b10-20rat} = q_{0.10rat} - q_{0.10-20}$, $q_{0.b10-20rat.ex} = q_{0.b10-20rat} - q_{0.15}$, $q_{0.b10-20rat.def} = q_{0.15} - q_{0.b10-20rat}$, $\sum q_{0.b10-20rat.ex} = \sum (q_{0.b10-20rat} - q_{0.15})\tau$.

As can be seen, the actual values of available booster refrigeration capacities $q_{0.b10-20rat}$ are mostly higher than the current requirement of $q_{0.15}$ for preconditioning outdoor air to 15 °C (Figure 3a). Accordingly, the current exceedances of the booster refrigeration capacities, $q_{0.b10-20rat.ex}$, in the majority offset the current deficit, $q_{0.b10-20rat.def}$, which is proven by the dominant rise in the summarized exceedance of booster refrigeration energy values $\sum q_{0.b10-20rat.ex}\tau$, except on a couple of days at the end of July (Figure 3b).

The practically constant summarized exceedance of the booster refrigeration energy values $\sum q_{0.b10-20rat.ex}\tau$ between the 10–13th and 20–26th July justifies that the daily values of deficit $\sum q_{0.b10-20rat.def}\tau$ are compensated by their values of reserved refrigeration energy $\sum q_{0.b10-20rat.ex}\tau$. However, the briefly lowering values $\sum q_{0.b10-20rat.ex}\tau$ within the 27–28th July indicate the presence of small daily refrigeration capacity deficit of $q_{0.20rat}$.
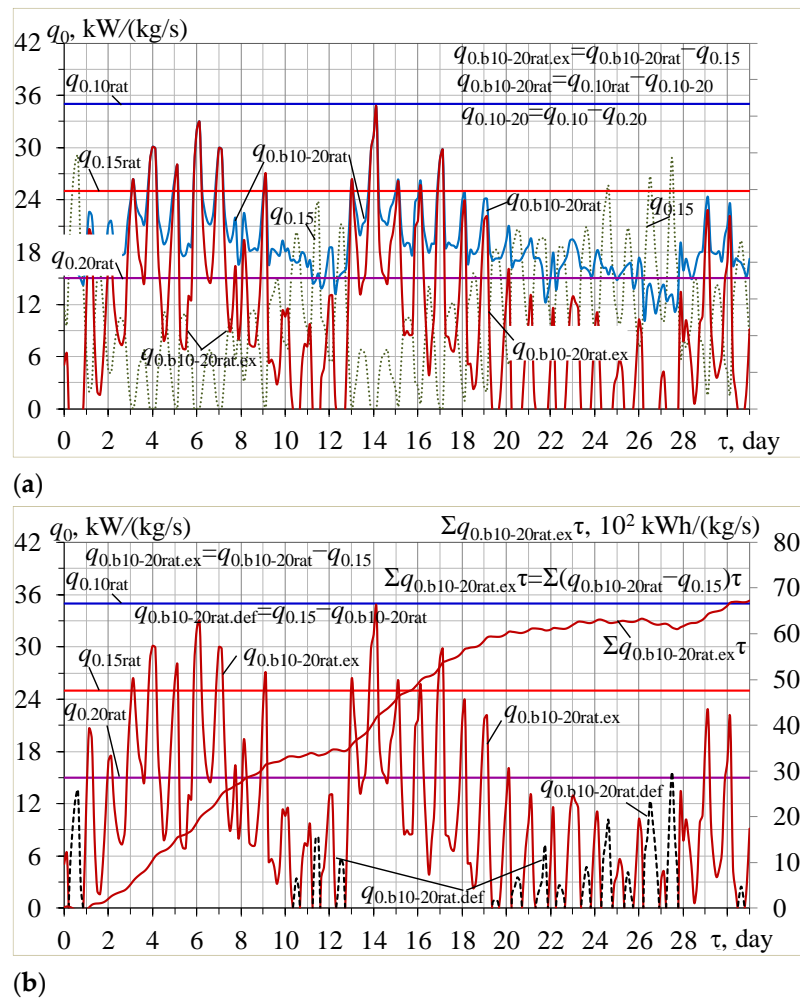
(**a**)

(**b**)

Figure 3. Rational values of refrigeration capacities $q_{0.10rat}$, $q_{0.15rat}$ and $q_{0.20rat}$ for conditioning outdoor air to 10 °C, 15 °C and 20 °C accordingly; actual refrigeration capacities $q_{0.15}$ needed for preconditioning air to 15 °C, and available booster refrigeration capacity $q_{0.b10-20rat}$ for preconditioning air and booster refrigeration capacity exceedance $q_{0.b10-20rat.ex}$ over $q_{0.15}$ (**a**), and its deficit $q_{0.b10-20rat.def}$, summarized monthly refrigeration energy exceedance $\sum q_{0.b10-20rat.ex}$ over $q_{0.15}$ (**b**): $q_{0.b10-20rat} = q_{0.10rat} - q_{0.10-20}$, $q_{0.b10-20rat.ex} = q_{0.b10-20rat} - q_{0.15}$, $q_{0.b10-20rat.def} = q_{0.15} - q_{0.b10-20rat}$, $\sum q_{0.b10-20rat.ex} = \sum(q_{0.b10-20rat} - q_{0.15})\tau$.

The continuously rising character of the available summarized exceedance of the booster refrigeration energy curve $\sum q_{0.b10-20rat.ex}$ confirms that the booster refrigeration energy enables it to cover the current need $q_{0.15}$ for preconditioning outdoor air to 15 °C instead of 20 °C, and to offset the actual deficit $q_{0.b10-20rat.def}$ by recuperating the daily excess of refrigeration energy $\sum q_{0.b10-20rat.ex}$ reserved at lowered current heat loads $q_{0.15}$, with a significant monthly exceedance of 6600 kWh/(kg/s) (Figure 3). The latter indicates the refrigeration energy reserve for reducing the installed booster refrigeration capacity from $q_{0.15rat}$ to $q_{0.20rat}$, and the total $q_{0.10rat}$ by the value of their difference $q_{0.15rat} - q_{0.20rat}$ = 10 kW/(kg/s) according to Figure 1.

Meanwhile, the booster refrigeration capacities $q_{0.b10-20opt}$, based on the optimal design value $q_{0.10opt}$, are not able to offset the current need $q_{0.15}$ for preconditioning outdoor air to 15 °C (Figure 4).
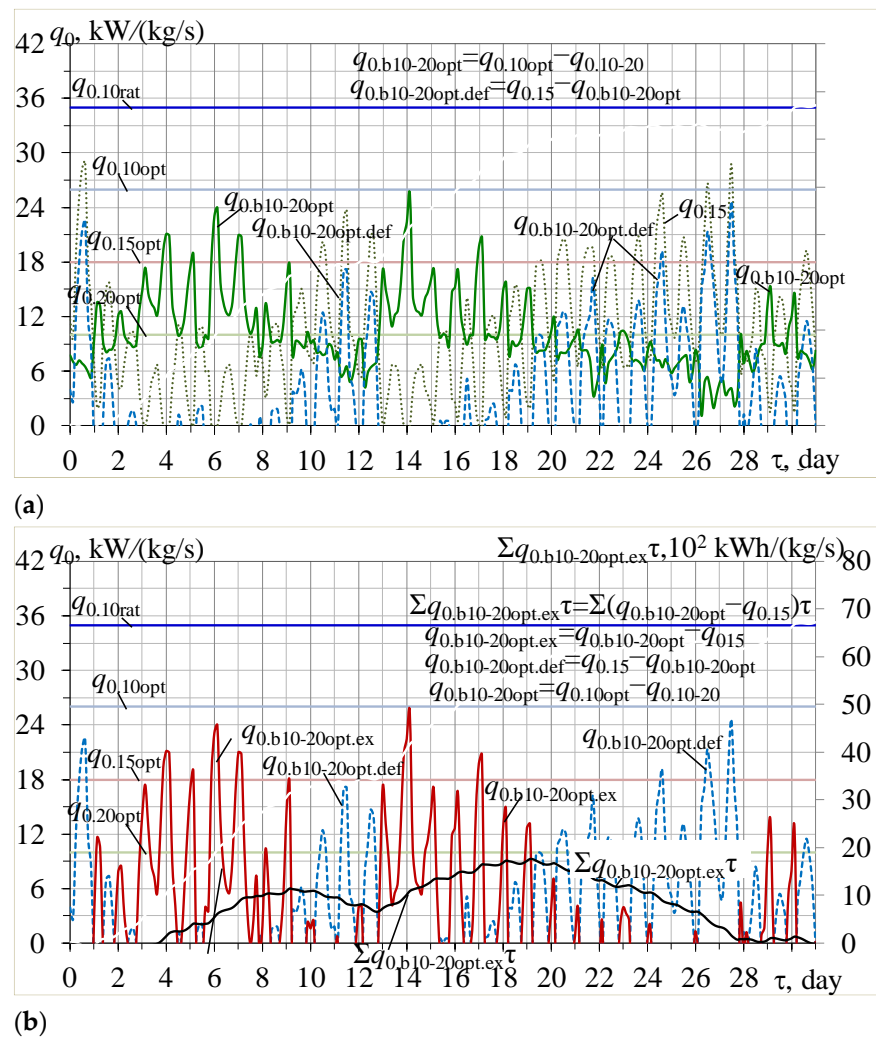
(a)

(b)

Figure 4. Optimal values of refrigeration capacities $q_{0.10opt}$, $q_{0.15opt}$ and $q_{0.20opt}$ for conditioning outdoor air to 10 °C, 15 °C and 20 °C accordingly; actual refrigeration capacities $q_{0.15}$ needed for preconditioning outdoor air to 15 °C; booster refrigeration capacity $q_{0.b10-20opt}$ and its deficit $q_{0.b10-20opt.def}$ compared to needed $q_{0.15}$ (**a**), booster refrigeration capacity exceedance $q_{0.b10-20opt.ex}$ over $q_{0.15}$ and summarized monthly refrigeration energy exceedance $\Sigma q_{0.b10-20opt.ex}$ (**b**).

The following correlations are used: $q_{0.b10-20opt} = q_{0.10opt} - q_{0.10-20}$, $q_{0.b10-20opt.ex} = q_{0.b10-20opt} - q_{0.15}$, $q_{0.b10-20opt.def} = q_{0.15} - q_{0.b10-20opt}$, $\Sigma q_{0.b10-20opt.ex} = \Sigma(q_{0.b10-20opt} - q_{0.15})\tau$.

As can be seen, the actual values of available booster refrigeration capacities $q_{0.b10-20opt}$ are lower than the current need $q_{0.15}$ within 10–13th and later 20th of July, which leads to considerable values of the current deficit $q_{0.b10-20opt.def}$ (Figure 4a). Accordingly, the current deficits $q_{0.b10-20opt.def}$ are comparable with the current exceedance of booster refrigeration capacities $q_{0.b10-20opt.ex}$ that is proven by alternating the rising and falling of the summarized exceedance of booster refrigeration energy values $\Sigma q_{0.b10-20opt.ex}\tau$ during July (Figure 4b).

Thus, in contrast to the rational value $q_{0.20rat}$, the optimal value $q_{0.20opt}$ is lower than the current need $q_{0.15}$ to be covered by daily reserved refrigeration energy $\Sigma q_{0.b10-20opt.ex}\tau$.

In order to approve such a preliminary conclusion, calculations of the current values of the available booster optimal refrigeration capacities $q_{0.b10-20opt}$ and corresponding summarized monthly refrigeration energy values $\Sigma q_{0.b10-20opt}\tau = \Sigma(q_{0.10opt} - q_{0.10-20})\tau$, compared with the current exceedances of booster rational refrigeration capacities $q_{0.b10-20rat.ex} = q_{0.b10-20rat} - q_{0.15}$, and corresponding summarized data on refrigeration energy $\Sigma q_{0.b10-20rat.ex}\tau = \Sigma(q_{0.b10-20rat} - q_{0.15})\tau$, are performed (Figure 5).
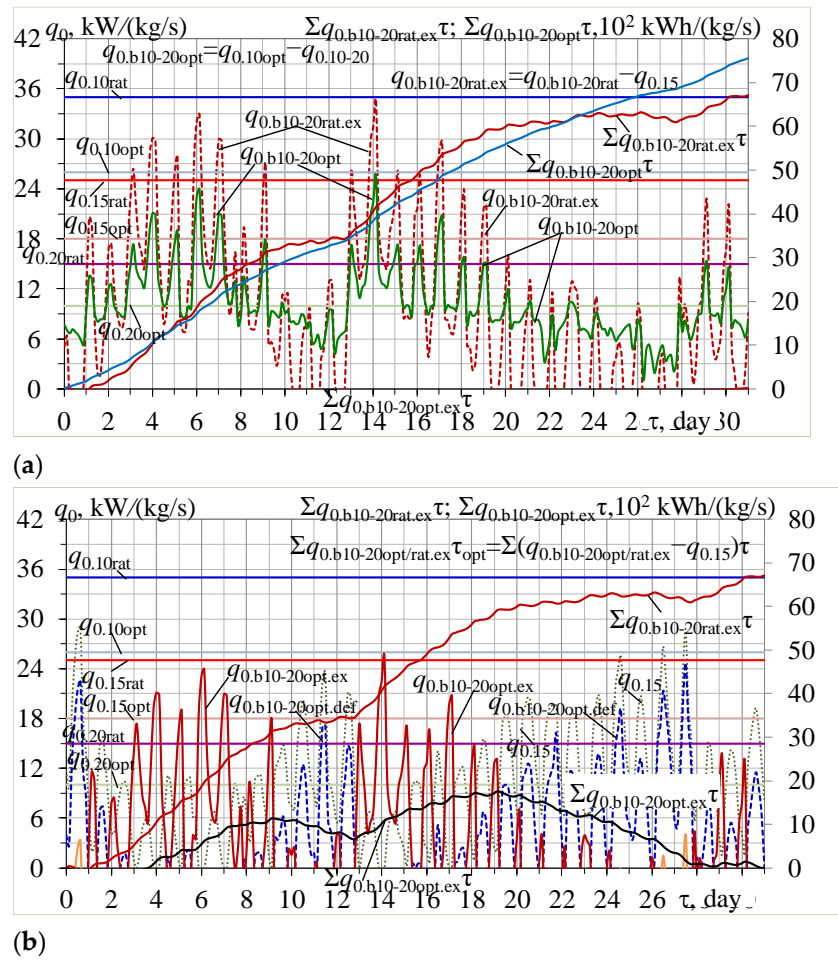
(a)

(b)

Figure 5. Current values of refrigeration capacities $q_{0.15}$ needed for preconditioning outdoor air to 15 °C; booster optimal refrigeration capacity $q_{0.b10-20opt}$ and corresponding summarized monthly refrigeration energy values $\Sigma q_{0.b10-20opt}\tau$, current exceedances of booster rational refrigeration capacities $q_{0.b10-20rat.ex}$ and corresponding summarized data $\Sigma q_{0.b10-20rat.ex}\tau$ (**a**), current booster optimal refrigeration capacity exceedance $q_{0.b10-20opt.ex}$ and its deficit $q_{0.b10-20opt.def}$, summarized booster refrigeration energy exceedance for optimal $\sum q_{0.b10-20opt.ex}$ and rational data $\sum q_{0.b10-20rat.ex}$ (**b**).

The following correlations are used: $q_{0.b10-20opt} = q_{0.10opt} - q_{0.10-20}$, $q_{0.b10-20rat} = q_{0.10rat} - q_{0.10-20}$, $q_{0.b10-20opt.ex} = q_{0.b10-20opt} - q_{0.15}$, $q_{0.b10-20opt.def} = q_{0.15} - q_{0.b10-20opt}$, $q_{0.b10-20rat.ex} = q_{0.b10-20rat} - q_{0.15}$, $\Sigma q_{0.b10-20opt}\tau = \Sigma(q_{0.10opt} - q_{0.10-20})\tau$, $\Sigma q_{0.b10-20opt.ex}\tau = \Sigma(q_{0.b10-20opt} - q_{0.15})\tau$, $\Sigma q_{0.b10-20rat.ex} = \Sigma(q_{0.b10-20rat} - q_{0.15})\tau$.

As Figure 5a shows, the values of available summarized monthly booster optimal refrigeration energy values $\Sigma q_{0.b10-20opt}\tau = \Sigma(q_{0.10opt} - q_{0.10-20})\tau$ are quite close to the summarized exceedances of the booster rational refrigeration energy $\Sigma q_{0.b10-20rat.ex}\tau = \Sigma(q_{0.b10-20rat} - q_{0.15})\tau$ which remain from the excessive refrigeration recuperation and are unavailable for further reducing the booster rational refrigeration energy. Proceeding from this data, we can conclude that in the general sense, the booster optimal refrigeration energy exceedance $\sum q_{0.b10-20opt.ex} = \sum(q_{0.b10-20opt} - q_{0.15})\tau$ is not enough to precondition outdoor air lower than 20 °C down to 15 °C; this is in contrast with the excessive booster rational refrigeration energy $\sum q_{0.b10-20rat}$, which is able to cover $q_{0.15}$, even with the rest $\sum q_{0.b10-20rat.ex} = \sum(q_{0.b10-20rat} - q_{0.15})\tau$.

The booster refrigeration capacities $q_{0.b10-20opt/rat} = q_{0.10opt/rat} - q_{0.10-20}$ and the values of their refrigeration capacity exceedance $q_{0.b10-20opt/rat.ex} = q_{0.b10-20opt/rat} - q_{0.15}$ over $q_{0.15}$ were calculated to approve this assumption (Figures 6 and 7).
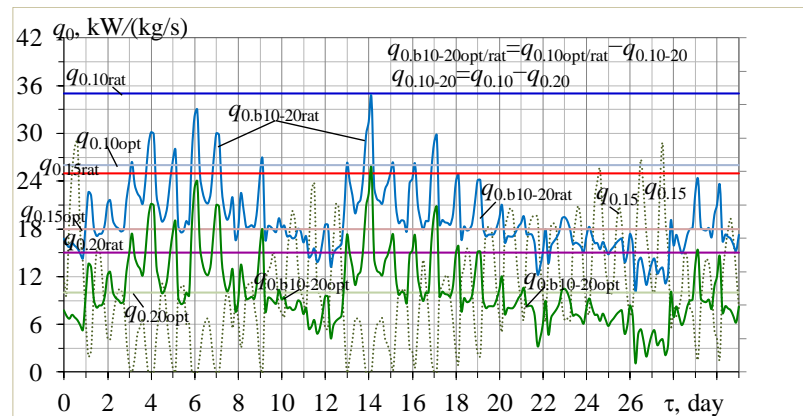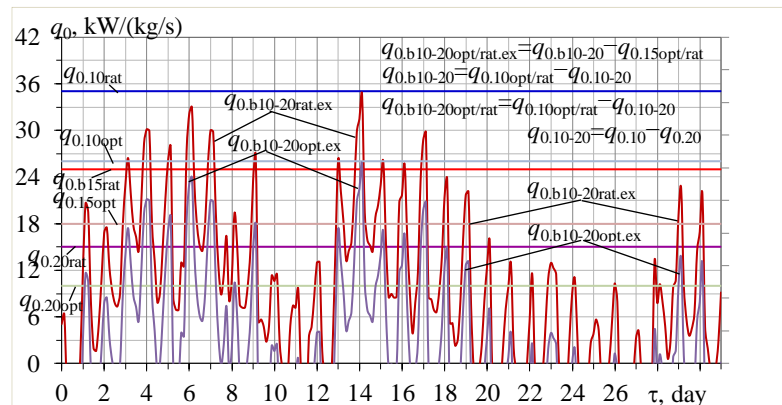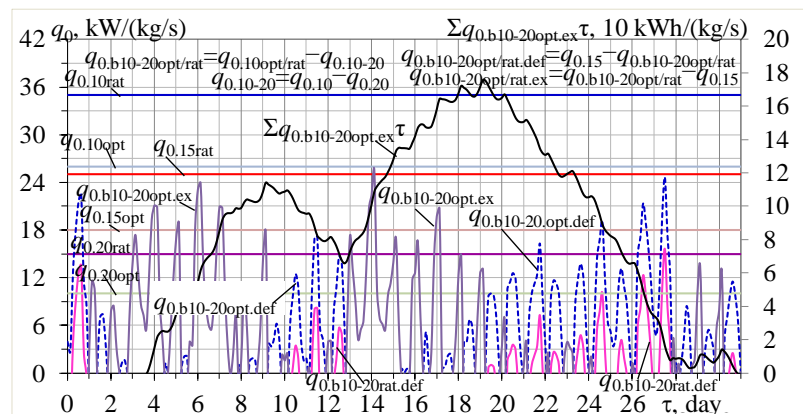
Figure 6. Actual values of refrigeration capacities $q_{0.15}$ needed for conditioning outdoor air to 15 °C, and booster refrigeration capacities $q_{0.b10-20opt}$ and $q_{0.b10-20rat}$ based on the optimal and rational design values $q_{0.10opt}$ and $q_{0.10rat}$ for conditioning outdoor air to 10 °C: $q_{0.b10-20opt} = q_{0.10opt} - q_{0.10-20}$; $q_{0.b10-20rat} = q_{0.10rat} - q_{0.10-20}$.

(**a**)

(**b**)

Figure 7. Actual values of booster refrigeration capacity exceedance $q_{0.b10-20opt.ex}$ and $q_{0.b10-20rat.ex}$ over $q_{0.15}$ (**a**) and its deficit $q_{0.b10-20opt.def}$ and $q_{0.b10-20rat.def}$ based on the optimal and rational design values $q_{0.10opt}$ and $q_{0.10rat}$ for conditioning outdoor air to 10 °C; summarized monthly refrigeration energy exceedance $\sum q_{0.b10-20opt.ex}$ over $q_{0.15}$; (**b**): $q_{0.b10-20rat} = q_{0.10rat} - q_{0.10-20}$, $q_{0.b10-20rat.ex} = q_{0.b10-20rat} - q_{0.15}$, $q_{0.b10-20opt.def} = q_{0.15} - q_{0.b10-20opt}$, $q_{0.b10-20rat.def} = q_{0.15} - q_{0.b10-20rat}$, $\sum q_{0.b10-20rat.ex} = \sum (q_{0.b10-20rat} - q_{0.15})\tau$, $\sum q_{0.b10-20opt.ex} = \sum (q_{0.b10-20opt} - q_{0.15})\tau$.

As may be seen, the actual values of available booster refrigeration capacities $q_{0.b10-20opt}$ are lower than the current need $q_{0.15}$ from 10–13th and later 20th of July, which leads to

considerable current deficit values of $q_{0.b10-20opt.def}$ (Figure 7a). Accordingly, the current deficits $q_{0.b10-20opt.def}$ are comparable with the current exceedances of the booster refrigeration capacities $q_{0.b10-20opt.ex}$ that are proven by alternating the rising and falling of the summarized exceedance of booster refrigeration energy values $\sum q_{0.b10-20opt.ex}\tau$ during July (Figure 7b).

Thus, in contrast to the rational value $q_{0.20rat}$, the optimal value $q_{0.20opt}$ is lower than the current need $q_{0.15}$ to be covered by the daily reserved refrigeration energy $\sum q_{0.b10-20opt.ex}\tau$.

As Figure 8 shows, the current values of required level of regulated load (LRL) of SRC in the ratio $q_{0.b10-20opt}/q_{0.10-20rat}$ fluctuate within the range of the required design nominal value $LRL_{nom} = q_{0.15rat}/q_{0.10rat}$, of about 0.7 to 0.3–0.2. The range of load, regulated by an SCR compressor, is characterized by the level of regulated load LRL as a ratio of the regulated load to the overall load $q_{0.10}$, including the unregulated load.
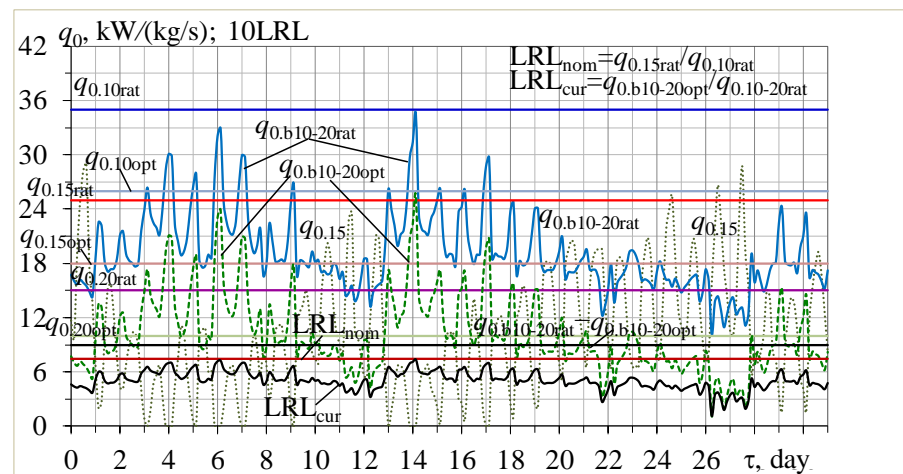

Figure 8. Actual refrigeration capacities $q_{0.15}$ needed for preconditioning outdoor air to 15 °C, booster refrigeration capacity $q_{0.b10-20opt}$ and $q_{0.b10-20rat}$ based on $q_{0.10opt}$ and $q_{0.10rat}$, the difference $q_{0.b10-20rat}$ $- q_{0.b10-20opt} = q_{0.10rat} - q_{0.10opt}$, current LRL_{cur} and nominal LRL_{nom}: $q_{0.b10-20rat} = q_{0.10rat} - q_{0.10-20}$, $q_{0.b10-20opt} = q_{0.10opt} - q_{0.10-20}$ $q_{0.b10-20rat.ex} = q_{0.b10-20rat} - q_{0.15}$, $q_{0.b10-20rat.def} = q_{0.15} - q_{0.b10-20rat}$, $\sum q_{0.b10-20rat.ex} = \sum(q_{0.b10-20rat} - q_{0.15})\tau$; $LRL_{nom} = q_{0.15rat}/q_{0.10rat}$; $LRL_{cur} = q_{0.b10-20opt}/q_{0.10-20rat}$; $q_{0.b10-20rat} - q_{0.b10-20opt} = q_{0.10rat} - q_{0.10opt}$.

Thus, the developed two methods of determining the optimal refrigeration capacity $q_{0.10opt}$ and its rational value $q_{0.10rat}$ as the second stage in the generalized designing methodology [84,85] make it possible to define not only the value of LRL_{nom}, but the range of the current values of LRL_{cur} fluctuation too.

As Figure 9 shows, the booster optimal refrigeration capacities $q_{0.b10-20opt}$ of $q_{0.10opt}$ are enough to cover current need $q_{0.20}$ for cooling air to 20 °C with considerable exceedance $q_{0.b10-20opt.ex20}$, but sometimes less than the current need $q_{0.15}$ for cooling air to 15 °C (Figure 8), when corresponding exceedance $q_{0.b10-20opt.ex15}$ drops to zero (Figure 9). The latter is also proven by the alternating the rising and falling of the summarized available exceedance of the booster optimal refrigeration energy values $\sum q_{0.b10-20opt.ex}\tau = \Sigma(q_{0.b10-20opt} - q_{0.15})\tau$ during July (Figure 9). There are opposite results for the summarized available exceedance of the booster rational refrigeration energy values $\sum q_{0.b10-20rat.ex}\tau = \Sigma(q_{0.b10-20rat} - q_{0.15})\tau$, characterized by a continuous rise that demonstrates that the booster rational refrigeration energy is able to cover the current need $q_{0.15}$ for preconditioning outdoor air to 15 °C instead of 20 °C; this is achieved by recuperating the daily excess of refrigeration energy $\sum q_{0.b10-20rat.ex}$ reserved at lower current heat loads $q_{0.15}$.
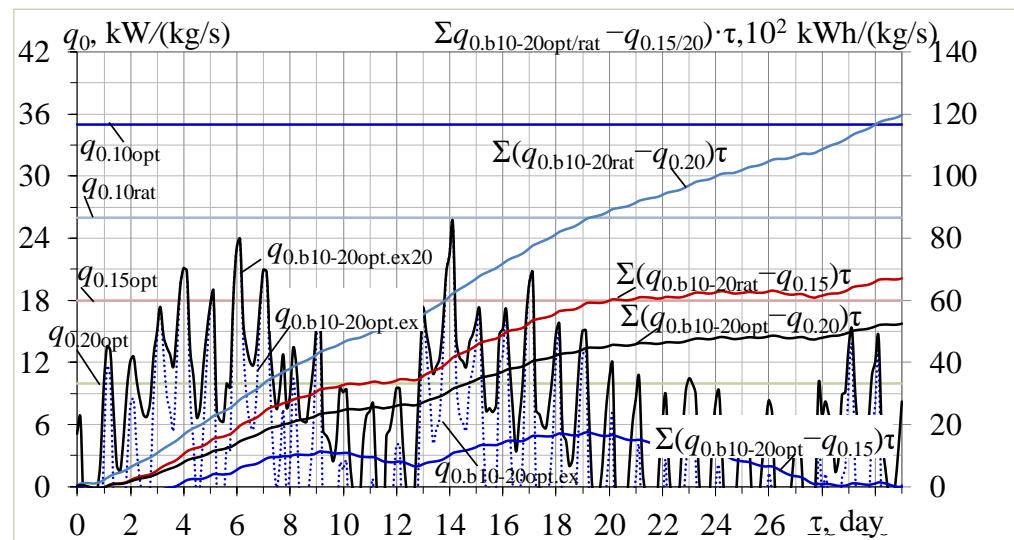
Figure 9. Actual values of booster optimal refrigeration capacity exceedance $q_{0.b10-20opt.ex}$ over $q_{0.15}$ and $q_{0.b10-20opt.ex20}$ over $q_{0.20}$; summarized monthly booster optimal refrigeration energy exceedances $\Sigma q_{0.b10-20opt.ex}\tau$ over $q_{0.15}$ and $\Sigma q_{0.b10-20opt.ex}\tau$ over $q_{0.20}$; summarized data on booster rational refrigeration energy $\Sigma q_{0.b10-20rat.ex}\tau$ over $q_{0.15}$ and $\Sigma q_{0.b10-20rat.ex20}\tau$ over $q_{0.20}$: $q_{0.b10-20opt.ex} = q_{0.b10-20opt} - q_{0.15}$; $q_{0.b10-20opt.ex20} = q_{0.b10-20opt} - q_{0.20}$; $\Sigma q_{0.b10-20opt.ex}\tau = \Sigma(q_{0.b10-20opt} - q_{0.15})\tau$; $\Sigma q_{0.b10-20opt.ex}\tau = \Sigma(q_{0.b10-20opt} - q_{0.20})\tau$; $\Sigma q_{0.b10-20rat.ex}\tau = \Sigma(q_{0.b10-20rat} - q_{0.15})\tau$; $\Sigma q_{0.b10-20rat.ex20}\tau = \Sigma(q_{0.b10-20rat} - q_{0.20})\tau$.

The practically constant summarized exceedance of the booster rational refrigeration energy values $\Sigma q_{0.b10-20rat.ex}\tau = \Sigma(q_{0.b10-20rat} - q_{0.15})\tau$ between 10–13th and 20–26th July justifies that daily values of the deficit are compensated by the values of reserved refrigeration energy $\Sigma q_{0.b10-20rat.ex}\tau$.

The similar character of the summarized exceedance of the booster optimal refrigeration energy values $\Sigma q_{0.b10-20opt.ex20}\tau = \Sigma(q_{0.b10-20opt} - q_{0.20})\tau$ indicates that operation of the compressor at optimal loads also requires refrigeration energy exceedance recuperation for booster air to be preconditioned to 20 °C.

The results of reduction in installed (design) refrigeration capacities through refrigeration energy exceedance recuperation, proceeding from optimal $q_{0.10opt}$ and rational $q_{0.10rat}$ values calculated for temperate climatic conditions in southern Ukraine, 2017, are presented in Figure 10.

As may be seen, the values of reduction in initial rational design specific refrigeration capacity due to optimal design $\Delta q_{0.10opt}$ and by refrigeration energy exceedance recuperation in booster air preconditioning to 15 °C $\Delta q_{0.15-20rat}$, resulting in reducing the rational value of design refrigeration capacity from $q_{0.15rat}$ to $q_{0.20rat}$, are nearly the same. However, the annual refrigeration energy generation according to current consumption $\Sigma(q_0 \cdot \tau)_{10opt}$ at the optimal refrigeration capacity $q_{0.10opt}$ is considerably lower than $\Sigma(q_0 \cdot \tau)_{10rat}$ at the rational refrigeration capacity $q_{0.10rat}$. In order to increase the annual refrigeration energy generation, as the primary criterion for the effect gained at optimal refrigeration capacity $q_{0.10opt}$, the refrigeration energy exceedance $\Sigma q_{0.b10-20opt}\tau = \Sigma(q_{0.10opt} - q_{0.10-20})\tau$ (Figure 8) has to be recuperated.
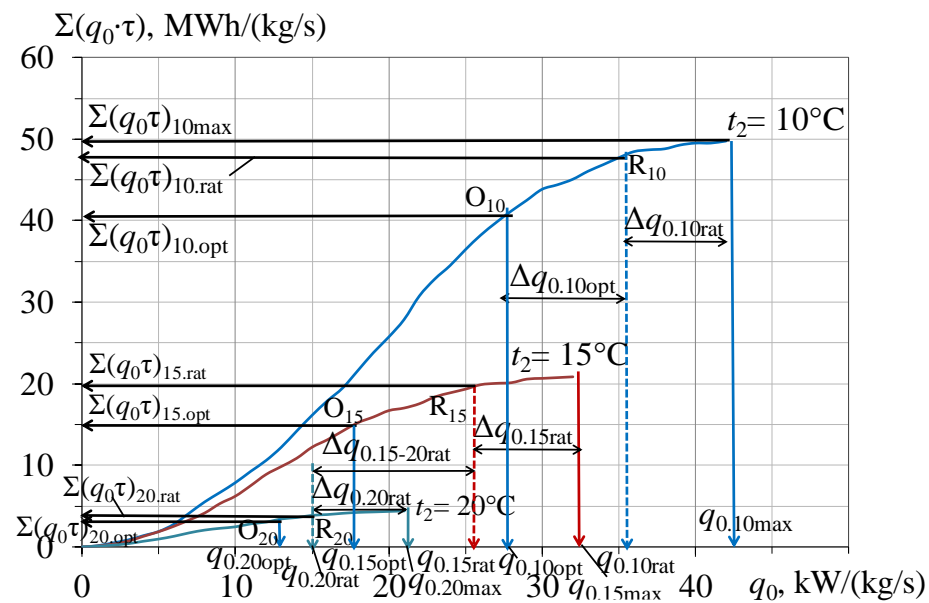
Figure 10. Specific annual refrigeration energy consumption $\sum(q_0 \cdot \tau)$; the rational $q_{0.10,15,20\text{rat}}$ and optimal $q_{0.10,15,20\text{opt}}$ values of design specific refrigeration capacity and their reductions $\Delta q_{0.10,15,20\text{rat/opt}}$ due to rational and optimal designing and refrigeration energy exceedance recuperation while conditioning air to $t_{a2} = 10$, 15 and 20 °C: $\Delta q_{0.10,15,20\text{rat}} = q_{0.10,15,20\text{max}} - q_{0.10,15,20\text{rat}}$; $\Delta q_{0.10\text{opt}} = q_{0.10\text{rat}} - q_{0.10\text{opt}}$; $\Delta q_{0.15-20\text{rat}} = q_{0.15\text{rat}} - q_{0.20\text{rat}}$.

4. Conclusions

The methods earlier developed by authors and aimed at determining the rational refrigeration capacity of ACS, providing the maximum annual refrigeration energy generation according to its consumption and its optimal value at the maximum rate of annual refrigeration energy increment, are adopted to reveal reserves for reducing the design refrigeration capacity of ACS through recuperation of the excessive refrigeration reserved at lowered loads to cover the current increased loads.

The modified methods of rational and optimal design of the ACS allow us to determine the initial ranges of changeable and unchangeable thermal loads, subsequently allowing us to partly stabilize the changeable load range through covering it with recuperated excessive refrigeration.

The artificial threshold air temperature, limiting the range of initially changeable loads stabilized through excessive refrigeration recuperation, is determined and proceeds from the rising character of the monthly summarized available exceedance of the refrigeration energy beyond its needs.

Such artificial thermal load stabilization through excessive refrigeration recuperation leads to a narrowed range of changeable loads and a reduction in the level of the regulated loads (LRL) of the SRC compressor.

Thus, the modified methods of rational and optimal design of the ACS allow us to determine the level of regulated loads (LRL) of the SRC, thus the load range of the compressor's operation was reduced more than 1.5 times. It has been shown that for temperate climatic conditions, the required LRL is about 0.5 with excessive refrigeration recuperation, versus 0.7 without refrigeration recuperation.

The further investigation is focused on the application of the approaches to designing two-stage outdoor ACS and the methods of defying the rational and optimal refrigeration capacities, developed initially for outdoor air conditioning, to realize two-stage principal in indoor subsystem with using the refrigeration excess gained in outdoor subsystem to reduce installed refrigeration capacity of indoor one.

Nomenclature and Units

ACS	Air conditioning system	
LL	Level of load	
LRL	Level of regulated load	
SRC	Speed regulated compressor	
VRF	Variable refrigerant flow	
Symbols and units		
b	Booster	
c_a	Specific heat of humid air	kJ/(kg·K)
G_a	Air mass flow rate	kg/s
Q_0	Total refrigeration capacity	kW
q_0	Specific refrigeration capacity (per unit air mass flow rate)	kW/(kg/s)
$q_0\,\tau$	Specific refrigeration energy (per unit air mass flow rate)	kW/(kg/s)
t	Air temperature	K, °C
ξ	Specific heat ratio of the total heat (latent and sensible) removed from air to sensible heat	
τ	Time interval	h
Δt	Temperature decrease	K, °C
$\sum(q_0\,\tau)$	Annual (monthly) specific refrigeration energy consumption (per unit air mass rate)	kWh/(kg/s)
Subscripts		
10, 15, 20	Air temperature	K, °C
a	Air	
amb	Ambient	
b	Booster	
max	Maximum	
opt	Optimal	
rat	Rational	

References

1. Gayeski, N.T.; Armstrong, P.R.; Norford, L.K. Predictive pre-cooling of thermo-active building systems with low-lift chillers. *HVAC&R Res.* **2012**, *18*, 1–16.
2. Southard, L.E.; Liu, X.; Spitler, J.D. Performance of HVAC systems at ASHRAE HQ. *ASHRAE J.* **2014**, *56*, 14–24.
3. Khliyeva, O.; Shestopalov, K.; Ierin, V.; Zhelezny, V.; Chen, G.; Gao, N. Environmental and energy comparative analysis of expediency of heat-driven and electrically-driven refrigerators for air conditioning application. *Appl. Therm. Eng.* **2022**, *219*, 119533. [CrossRef]
4. Forduy, S.; Radchenko, A.; Kuczynski, W.; Zubarev, A.; Konovalov, D. Enhancing the fuel efficiency of gas engines in integrated energy system by chilling cyclic air. In *InterPartner-2019, Proceedings of the Grabchenko's International Conference on Advanced Manufacturing Processes, Odessa, Ukraine, 10–13 September 2019*; Tonkonogyi, V., Ivanov, V., Trojanowska, J., Oborskyi, G., Edl, M., Kuric, I., Pavlenko, I., Dasic, P., Eds.; Lecture Notes in Mechanical Engineering; Springer: Cham, Switzerland, 2020; pp. 500–509. [CrossRef]
5. Radchenko, N.; Radchenko, A.; Tsoy, A.; Mikielewicz, D.; Kantor, S.; Tkachenko, V. Improving the efficiency of railway conditioners in actual climatic conditions of operation. *AIP Conf. Proc.* **2020**, *2285*, 030072.

6. Radchenko, A.; Radchenko, M.; Trushliakov, E.; Kantor, S.; Tkachenko, V. Statistical method to define rational heat loads on railway air conditioning system for changeable climatic conditions. In Proceedings of the 5th International Conference on Systems and Informatics, ICSAI 2018, Nanjing, China, 10–12 November 2018; pp. 1294–1298. [CrossRef]

7. Radchenko, M.; Mikielewicz, D.; Andreev, A.; Vanyeyev, S.; Savenkov, O. Efficient ship engine cyclic air cooling by turboexpander chiller for tropical climatic conditions. In *Integrated Computer Technologies in Mechanical Engineering—2020*; Nechyporuk, M., Pavlikov, V., Kritskiy, D., Eds.; Lecture Notes in Networks and Systems; Springer: Cham, Switzerland, 2021; Volume 188, pp. 498–507.

8. Yang, Z.; Radchenko, R.; Radchenko, M.; Radchenko, A.; Kornienko, V. Cooling potential of ship engine intake air cooling and its realization on the route line. *Sustainability* **2022**, *14*, 15058. [CrossRef]

9. Kornienko, V.; Radchenko, R.; Radchenko, M.; Radchenko, A.; Pavlenko, A.; Konovalov, D. Cooling cyclic air of marine engine with water-fuel emulsion combustion by exhaust heat recovery chiller. *Energies* **2022**, *15*, 248. [CrossRef]

10. Yang, Z.; Konovalov, D.; Radchenko, M.; Radchenko, R.; Kobalava, H.; Radchenko, A.; Kornienko, V. Analyzing the efficiency of thermopressor application for combustion engine cyclic air cooling. *Energies* **2022**, *15*, 2250. [CrossRef]

11. Shukla, A.K.; Sharma, A.; Sharma, M.; Mishra, S. Performance improvement of simple gas turbine cycle with vapor compression inlet air cooling. *Mater. Today Proc.* **2018**, *5*, 19172–19180. [CrossRef]

12. Tarasenko, O.I.; Tarasenko, A.O.; Radchenko, M.; Scurtu, I.C.; Volintiru, O.N.; Sichko, V. Digital regulation of gas turbine engine on start modes. *IOP Conf.Ser. Earth Environ. Sci.* **2022**, *968*, 012009. [CrossRef]

13. Radchenko, A.; Scurtu, I.-C.; Radchenko, M.; Forduy, S.; Zubarev, A. Monitoring the efficiency of cooling air at the inlet of gas engine in integrated energy system. *Therm. Sci.* **2022**, *26*, 185–194. [CrossRef]

14. Radchenko, A.; Radchenko, M.; Koshlak, H.; Radchenko, R.; Forduy, S. Enhancing the efficiency of integrated energy system by redistribution of heat based of monitoring data. *Energies* **2022**, *15*, 8774. [CrossRef]

15. Radchenko, A.; Radchenko, N.; Tsoy, A.; Portnoi, B.; Kantor, S. Increasing the efficiency of gas turbine inlet air cooling in actual climatic conditions of Kazakhstan and Ukraine. *AIP Conf. Proc.* **2020**, *2285*, 030071. [CrossRef]

16. Mohapatra, A.K. Comparative analysis of inlet air cooling techniques integrated to cooled gas turbine plant. *J. Energy Inst.* **2015**, *88*, 344–358. [CrossRef]

17. Suamir, I.N.; Tassou, S.A. Performance evaluation of integrated trigeneration and CO_2 refrigeration systems. *Appl. Therm. Eng.* **2013**, *50*, 1487–1495. [CrossRef]

18. Rocha, M.S.; Andreos, R.; Simões-Moreira, J.R. Performance tests of two small trigeneration pilot plants. *Appl. Therm. Eng.* **2012**, *41*, 84–91. [CrossRef]

19. Bai, Z.; Liu, Q.; Gong, L.; Lei, J. Application of a mid-/low-temperature solar thermochemical technology in the distributed energy system with cooling, heating and power production. *Appl. Energy* **2019**, *253*, 113491. [CrossRef]

20. Yu, Z.; Shevchenko, S.; Radchenko, M.; Shevchenko, O.; Radchenko, A. Methodology of Designing Sealing Systems for Highly Loaded Rotary Machines. *Sustainability* **2022**, *14*, 15828. [CrossRef]

21. Yang, Z.; Kornienko, V.; Radchenko, M.; Radchenko, A.; Radchenko, R.; Pavlenko, A. Capture of pollutants from exhaust gases by low-temperature heating surfaces. *Energies* **2022**, *15*, 120. [CrossRef]

22. Konovalov, D.; Radchenko, M.; Kobalava, H.; Radchenko, A.; Radchenko, R.; Kornienko, V.; Maksymov, V. Research of characteristics of the flow part of an aerothermopressor for gas turbine intercooling air. *Proc. Inst. Mech. Eng. Part A J. Power Energy* **2021**, *236*, 634–646. [CrossRef]

23. Yang, Z.; Kornienko, V.; Radchenko, M.; Radchenko, A.; Radchenko, R. Research of Exhaust Gas Boiler Heat Exchange Surfaces with Reduced Corrosion when Water-fuel Emulsion Combustion. *Sustainability* **2022**, *14*, 11927. [CrossRef]

24. Yang, Z.; Korobko, V.; Radchenko, M.; Radchenko, R. Improving thermoacoustic low temperature heat recovery systems. *Sustainability* **2022**, *14*, 12306. [CrossRef]

25. Tarasova, V.; Kuznetsov, M.; Kharlampidi, D.; Kostikov, A. Development of a vacuum-evaporative thermotransformer for the cooling system at a nuclear power plant. *East. -Eur. J. Enterp. Technol.* **2019**, *4*, 45–56. [CrossRef]

26. Shukla, A.K.; Singh, O. Thermodynamic investigation of parameters affecting the execution of steam injected cooled gas turbine based combined cycle power plant with vapor absorption inlet air cooling. *Appl. Therm. Eng.* **2017**, *122*, 380–388. [CrossRef]

27. Radchenko, A.; Radchenko, M.; Mikielewicz, D.; Pavlenko, A.; Radchenko, R.; Forduy, S. Energy saving in trigeneration plant for food industries. *Energies* **2022**, *15*, 1163. [CrossRef]

28. Radchenko, M.; Radchenko, A.; Mikielewicz, D.; Kosowski, K.; Kantor, S.; Kalinichenko, I. Gas turbine intake air hybrid cooling systems and their rational designing. In Proceedings of the V International Scientific and Technical Conference Modern Power Systems and Units (MPSU 2021). E3S Web of Conferences, Kraków, Poland, 19–21 May 2021; Volume 323, p. 00030. [CrossRef]

29. Khliyeva, O.; Zhelezny, V.; Lukianov, T.; Lukianov, N.; Semenyuk, V.; Moreir, A.L.N.; Murshed, S.M.S.; Palomo del Barrio, E.; Nikulin, N. A new approach for predicting the pool boiling heat transfer coefficient of refrigerant R141b and its mixtures with surfactant and nanoparticles using experimental data. *J. Therm. Anal. Calorim.* **2020**, *142*, 2327–2339. [CrossRef]

30. Zhelezny, V.; Khliyeva, O.; Lukianov, M.; Motovoy, I.; Ivchenko, D.A.; Faik, A.; Grosu, Y.; Nikulin, A.; Moreira, A.L.N. Thermodynamic properties of isobutane/mineral compressor oil and isobutane/mineral compressor oil/fullerenes C60 solutions. *Int. J. Refrig.* **2019**, *106*, 153–162. [CrossRef]

31. Yang, Z.; Radchenko, M.; Radchenko, A.; Mikielewicz, D.; Radchenko, R. Gas turbine intake air hybrid cooling systems and a new approach to their rational designing. *Energies* **2022**, *15*, 1512827. [CrossRef]

32. Ierin, V.; Chen, G.; Volovyk, O.; Shestopalov, K. Hybrid two—Stage CO_2 transcritical mechanical compression—Ejector cooling cycle: Thermodynamic analysis and optimization. *Int. J. Refrig.* **2021**, *132*, 45–55. [CrossRef]
33. Radchenko, M.; Radchenko, A.; Radchenko, R.; Kantor, S.; Konovalov, D.; Kornienko, V. Rational loads of turbine inlet air absorption-ejector cooling systems. *Proc. Inst. Mech. Eng. Part A J. Power Energy* **2021**, *236*, 450–462. [CrossRef]
34. Radchenko, R.; Radchenko, N.; Tsoy, A.; Forduy, S.; Zybarev, A.; Kalinichenko, I. Utilizing the heat of gas module by an absorption lithium-bromide chiller with an ejector booster stage. In Proceedings of the AIP Conference Proceedings 2020, Coimbatore, India, 17–18 July 2020; AIP Publishing LLC: Melville, NY, USA, 2020; Volume 2285, p. 030084. [CrossRef]
35. Ghatos, S.; Taha-Janan, M.; Mehdari, A. Thermodynamic model of a single stage H_2O-LiBr absorption cooling. In Proceedings of the E3S Web of Conferences, Kenitra, Morocco, 25–27 December 2021; EDP Sciences: Les Ulis, France, 2021; Volume 234, p. 00091.
36. Kalhori, S.B.; Rabiei, H.; Mansoori, Z. Mashad trigeneration potential–An opportunity for CO_2 abatement in Iran. *Energy Conv. Manag.* **2012**, *60*, 106–114. [CrossRef]
37. Radchenko, R.; Kornienko, V.; Pyrysunko, M.; Bogdanov, M.; Andreev, A. Enhancing the Efficiency of Marine Diesel Engine by Deep Waste Heat Recovery on the Base of Its Simulation Along the Route Line. In *Integrated Computer Technologies in Mechanical Engineering (ICTM 2019)*; Nechyporuk, M., Pavlikov, V., Kritskiy, D., Eds.; Advances in Intelligent Systems and Computing (2020); Springer: Cham, Switzerland, 2020; Volume 1113, pp. 337–350. [CrossRef]
38. Radchenko, N.I. On reducing the size of liquid separators for injector circulation plate freezers. *Aust. Refrig. Air Cond. Heat.* **1986**, *40*, 34–36. [CrossRef]
39. Chen, G.; Zhelezny, V.; Khliyeva, O.; Shestopalov, K.; Ierin, V. Ecological and energy efficiency analysis of ejector and vapor compression air conditioners. *Int. J. Refrig.* **2017**, *74*, 127–135. [CrossRef]
40. Chen, G.; Ierin, V.; Volovyk, O.; Shestopalov, K. An improved cascade mechanical compression—Ejector cooling cycle. *Energy* **2019**, *170*, 459–470. [CrossRef]
41. Shubenko, A.; Babak, M.; Senetskyi, O.; Tarasova, V.; Goloshchapov, V.; Senetska, D. Economic assessment of the modernization perspectives of a steam turbine power unit to the ultra-supercritical operation conditions. *Int. J. Energy Res.* **2022**, *46*, 23530–23537. [CrossRef]
42. Fan, C.; Pei, D.; Wei, H. A novel cascade energy utilization to improve efficiency of double reheat cycle. *Energy Convers. Manag.* **2018**, *171*, 1388–1396. [CrossRef]
43. Trushliakov, E.; Radchenko, M.; Radchenko, A.; Kantor, S.; Zongming, Y. Statistical Approach to Improve the Efficiency of Air Conditioning System Performance in Changeable Climatic Conditions. In Proceedings of the 5th International Conference on Systems and Informatics, ICSAI 2018, Nanjing, China, 10–12 November 2018; pp. 256–260. [CrossRef]
44. Radchenko, A.; Mikielewicz, D.; Radchenko, M.; Forduy, S.; Rizun, O.; Khaldobin, V. Innovative combined in-cycle trigeneration technologies for food industries. In Proceedings of the V International Scientific and Technical Conference Modern Power Systems and Units (MPSU 2021), E3S Web of Conferences, Kraków, Poland, 19–21 May 2021; Volume 323, p. 00029. [CrossRef]
45. Khatri, R.; Joshi, A. Energy performance comparison of inverter based variable refrigerant flow unitary AC with constant volume unitary AC. *Energy Procedia* **2017**, *109*, 18–26. [CrossRef]
46. Park, D.Y.; Yun, G.; Kim, K.S. Experimental evaluation and simulation of a variable refrigerant-flow (VRF) air-conditioning system with outdoor air processing unit. *Energy Build* **2017**, *146*, 122–140. [CrossRef]
47. Thornton, B.; Wagner, A. Variable Refrigerant Flow Systems. Seattle WA: Pacific Northwest National Laboratory. 2012. Available online: http://www.gsa.gov/portal/mediaId/197399/fileName/GPG_Variable_Refrigerant_Flow_12-2012.action (accessed on 19 January 2020).
48. Chen, J.; Xie, W. Analysis on load-undertaking of fan coil unit with fresh air system. *Adv. Mater. Res.* **2013**, *614*, 678–681. [CrossRef]
49. Zhu, Y.; Jin, X.; Du, Z.; Fang, X.; Fan, B. Control and energy simulation of variable refrigerant flow air conditioning system combined with outdoor air processing unit. *Appl. Therm. Eng.* **2014**, *64*, 385–395. [CrossRef]
50. Lee, J.H.; Yoon, H.J.; Im, P.; Song, Y.H. Verification of energy reduction effect through control optimization of supply air temperature in VRF-OAP system. *Energies* **2018**, *11*, 49. [CrossRef]
51. Lee, Y.; Kim, W. Development of an Optimal Start Control Strategy for a Variable Refrigerant Flow (VRF). *Syst. Energ.* **2021**, *14*, 271. [CrossRef]
52. Liu, C.; Zhao, T.; Zhang, J. Operational electricity consumption analyze of VRF air conditioning system and air conditioning system based on building energy monitoring and management system. *Procedia Eng.* **2015**, *121*, 1856–1863. [CrossRef]
53. Radchenko, N. A concept of the design and operation of heat exchangers with change of phase. *Arch. Thermodyn.* **2004**, *25*, 3–19.
54. Wajs, J.; Mikielewicz, D.; Jakubowska, B. Performance of the domestic micro ORC equipped with the shell-and-tube condenser with minichannels. *Energy* **2018**, *157*, 853–861. [CrossRef]
55. Pavlenko, A. Energy conversion in heat and mass transfer processes in boiling emulsions. *Therm. Sci. Eng. Prog.* **2020**, *15*, 00439. [CrossRef]
56. Pavlenko, A. Change of emulsion structure during heating and boiling. *Int. J. Energy A Clean Environ.* **2019**, *20*, 291–302. [CrossRef]
57. Kruzel, M.; Bohdal, T.; Dutkowski, K.; Kuczyński, W.; Chliszcz, K. Current Research Trends in the Process of Condensation of Cooling Zeotropic Mixtures in Compact Condensers. *Energies* **2022**, *15*, 2241. [CrossRef]
58. Kuczyński, W.; Kruzel, M.; Chliszcz, K. A Regressive Model for Periodic Dynamic Instabilities during Condensation of R1234yf and R1234ze Refrigerants. *Energies* **2022**, *15*, 2117. [CrossRef]

59. Kruzel, M.; Bohdal, T.; Dutkowski, K.; Radchenko, M. The Effect of Microencapsulated PCM Slurry Coolant on the Efficiency of a Shell and Tube Heat Exchanger. *Energies* **2022**, *15*, 5142. [CrossRef]

60. Dutkowski, K.; Kruzel, M. Microencapsulated PCM slurries' dynamic viscosity experimental investigation and temperature dependent prediction model. *Int. J. Heat Mass Transf.* **2019**, *145*, 118741. [CrossRef]

61. Kuczyński, W.; Kruzel, M.; Chliszcz, K. Regression Model of Dynamic Pulse Instabilities during Condensation of Zeotropic and Azeotropic Refrigerant Mixtures R404A, R448A and R507A in Minichannels. *Energies* **2022**, *15*, 1789. [CrossRef]

62. Pavlenko, A.M.; Koshlak, H. Application of thermal and cavitation effects for heat and mass transfer process intensification in multicomponent liquid media. *Energies* **2021**, *14*, 7996. [CrossRef]

63. Dąbrowski, P.; Klugmann, M.; Mikielewicz, D. Channel Blockage and Flow Maldistribution during Unsteady Flow in a Model Microchannel Plate heat Exchanger. *J. Appl. Fluid Mech.* **2019**, *12*, 1023–1035. [CrossRef]

64. Dąbrowski, P.; Klugmann, M.; Mikielewicz, D. Selected studies of flow maldistribution in a minichannel plate heat exchanger. *Arch. Thermodyn.* **2017**, *38*, 135–148. [CrossRef]

65. Kumar, R.; Singh, G.; Mikielewicz, D. A New Approach for the Mitigating of Flow Maldistribution in Parallel Microchannel Heat Sink. *J. Heat Transf.* **2018**, *140*, 72401–72410. [CrossRef]

66. Kumar, R.; Singh, G.; Mikielewicz, D. Numerical Study on Mitigation of Flow Maldistribution in Parallel Microchannel Heat Sink: Channels Variable Width Versus Variable Height Approach. *J. Electron. Packag.* **2019**, *141*, 21009–21011. [CrossRef]

67. Qian, Z.; Wang, Q.; Cheng, J.; Deng, J. Simulation investigation on inlet velocity profile and configuration parameters of louver fin. *Appl. Therm. Eng.* **2018**, *138*, 173–182. [CrossRef]

68. Yaïci, W.; Ghorab, M.; Entchev, E. 3D CFD study of the effect of inlet air flow maldistribution on plate-fin-tube heat exchanger design and thermal–hydraulic performance. *Int. J. Heat Mass Transf.* **2016**, *101*, 527–541. [CrossRef]

69. Radchenko, N.; Trushliakov, E.; Radchenko, A.; Tsoy, A.; Shchesiuk, O. Methods to determine a design cooling capacity of ambient air conditioning systems in climatic conditions of Ukraine and Kazakhstan. *AIP Conf. Proc.* **2020**, *2285*, 030074. [CrossRef]

70. Radchenko, R.; Kornienko, V.; Radchenko, M.; Mikielewicz, D.; Andreev, A.; Kalinichenko, I. Cooling intake air of marine engine with water-fuel emulsion combustion by ejector chiller. In Proceedings of the V International Scientific and Technical Conference Modern Power Systems and Units (MPSU 2021), E3S Web of Conferences, Kraków, Poland, 19–21 May 2021; Volume 323, p. 00031. [CrossRef]

71. Yu, Z.; Løvås, T.; Konovalov, D.; Trushliakov, E.; Radchenko, M.; Kobalava, H.; Radchenko, R.; Radchenko, A. Investigation of thermopressor with incomplete evaporation for gas turbine intercooling systems. *Energies* **2023**, *16*, 20. [CrossRef]

72. Konovalov, D.; Trushliakov, E.; Radchenko, M.; Kobalava, G.; Maksymov, V. Research of the aerothermopresor cooling system of charge air of a marine internal combustion engine under variable climatic conditions of operation. In *InterPartner-2019, Proceedings of the Grabchenko's International Conference on Advanced Manufacturing Processes, Odessa, Ukraine, 10–13 September 2019*; Tonkonogyi, V., Ivanov, V., Trojanowska, J., Oborskyi, G., Edl, M., Kuric, I., Pavlenko, I., Dasic, P., Eds.; Lecture Notes in Mechanical Engineering; Springer: Cham, Switzerland, 2020; pp. 520–529. [CrossRef]

73. Konovalov, D.; Radchenko, R.; Kobalava, H.; Zubarev, A.; Sviridov, V.; Kornienko, V. Analysing the efficiency of thermopressor application in the charge air cooling system of combustion engine. In Proceedings of the V International Scientific and Technical Conference Modern Power Systems and Units (MPSU 2021), E3S Web of Conferences, Kraków, Poland, 19–21 May 2021; Volume 323, p. 00017. [CrossRef]

74. Kornienko, V.; Radchenko, M.; Radchenko, R.; Kruzel, M.; Konovalov, D.; Andreev, A. Absorption of pollutants from exhaust gases by low-temperature heating surfaces. In Proceedings of the V International Scientific and Technical Conference Modern Power Systems and Units (MPSU 2021), E3S Web of Conferences, Kraków, Poland, 19–21 May 2021; Volume 323, p. 00018. [CrossRef]

75. Dhaka, S.; Mathur, J.; Garg, V. Combined effect of energy efficiency measures and thermal adaptation on air conditioned building in warm climatic conditions of India. *Energy Build.* **2012**, *55*, 351–360. [CrossRef]

76. Fumo, N.; Mago, P.J.; Smith, A.D. Analysis of combined cooling, heating, and power systems operating following the electric load and following the thermal load strategies with no electricity export. *Proc. Inst. Mech. Eng. Part A J. Power Energy* **2011**, *225*, 1016–1025. [CrossRef]

77. Cardona, E.; Piacentino, A. A methodology for sizing a trigeneration plant in mediterranean areas. *Appl. Therm. Eng.* **2003**, *23*, 15. [CrossRef]

78. Ortiga, J.; Bruno, J.C.; Coronas, A. Operational optimization of a complex trigeneration system connected to a district heating and cooling network. *Appl. Therm. Eng.* **2013**, *50*, 1536–1542. [CrossRef]

79. Kavvadias, K.C.; Tosios, A.P.; Maroulis, Z.B. Design of a combined heating, cooling and power system: Sizing, operation strategy selection and parametric analysis. *Energy Convers Manag.* **2010**, *51*, 833–845. [CrossRef]

80. Freschi, F.; Giaccone, L.; Lazzeroni, P.; Repetto, M. Economic and environmental analysis of a trigeneration system for food-industry: A case study. *Appl. Energy* **2013**, *107*, 157–172. [CrossRef]

81. Radchenko, M.; Radchenko, A.; Mikielewicz, D.; Radchenko, R.; Andreev, A. A novel degree-hour method for rational design loading. *Proc. Inst. Mech. Eng. Part A J. Power Energy* **2022**. [CrossRef]

82. Radchenko, A.; Trushliakov, E.; Kosowski, K.; Mikielewicz, D.; Radchenko, M. Innovative turbine intake air cooling systems and their rational designing. *Energies* **2020**, *13*, 6201. [CrossRef]

83. Radchenko, M.; Bohdal, T.; Radchenko, A.; Trushliakov, E.; Tkachenko, V.; Zielikov, O.; Tzaran, F. Alternative variable refrigerant flow (VRF) air conditioning systems with rational distribution of thermal load. In Proceedings of the V International Scientific and Technical Conference Modern Power Systems and Units (MPSU 2021), E3S Web of Conferences, Kraków, Poland, 19–21 May 2021; Volume 323, p. 00028. [CrossRef]
84. Radchenko, M.; Radchenko, A.; Trushliakov, E.; Pavlenko, A.M.; Radchenko, R. Advanced method of variable refrigerant flow (VRF) systems designing to forecast on site operation. Part 1: General approaches and criteria. *Energies* **2023**, *16*, 1381. [CrossRef]
85. Radchenko, M.; Radchenko, A.; Trushliakov, E.; Koshlak, H.; Radchenko, R. Advanced method of variable refrigerant flow (VRF) systems designing to forecast on site operation. Part 2: Phenomenological simulation to recuperate refrigeration energy. *Energies* **2023**, *16*, 1922. [CrossRef]